ACS Macro Letters

Letter

pubs.acs.org/macroletters

Supramolecular Fluorescent Nanoparticles for Targeted Cancer Imaging

Ruijiao Dong,[†] Hongying Chen,[‡] Dali Wang,[†] Yuanyuan Zhuang,[†] Lijuan Zhu,[†] Yue Su,[†] Deyue Yan,[†] and Xinyuan Zhu*[,†,§]

[†]School of Chemistry and Chemical Engineering, State Key Laboratory of Metal Matrix Composites, Shanghai Jiao Tong University, 800 Dongchuan Road, Shanghai 200240, P. R. China

[‡]Department of Oral and Maxillofacial Surgery, The First Affiliated Hospital of Harbin Medical University, 23 Youzheng Street, Nangang District, Harbin 150001, P. R. China

[§]Instrumental Analysis Center, Shanghai Jiao Tong University, 800 Dongchuan Road, Shanghai 200240, P. R. China

Supporting Information

ABSTRACT: By a combination of excellent fluorescent performance with smart targeting capability for cancer-specific delivery, a promising class of calcein-based supramolecular fluorescent nanoparticles has been successfully prepared via a "bricks and mortar" strategy. Through tuning the molar ratio of adamantane-functionalized calcein (CA-AD)/β-cyclodextrin-grafted branched polyethylenimine (PEI-CD), the size of these fluorescent nanoparticles can be effectively controlled. Importantly, the β-cyclodextrin/adamantane (β-CD/AD = 1/1) host–guest interaction dramatically suppresses the $\pi-\pi$ stacking and fluorescence self-quenching of calcein chromophores in water, leading to the formation of highly fluorescent nanoparticles. By introduction of the folate receptor, these fluorescent nanoparticles exhibit excellent cancer imaging efficiency.

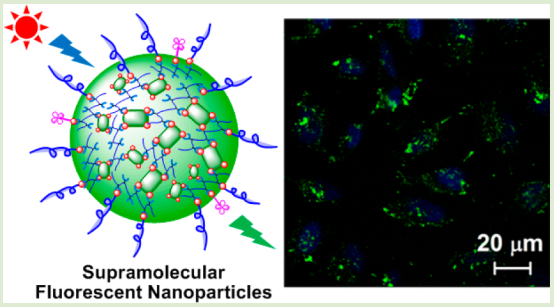

The construction of well-defined nanostructures such as nanoparticles, nanorods and nanowires with controllable morphologies and sizes has attracted considerable interest.[1] Due to its dynamic self-assembly and molecular recognition, supramolecular chemistry provides a powerful and facile approach for the preparation of ordered nanomaterials from molecular building blocks.[2] Among various supramolecular conjugated systems, the irregular aggregates or insoluble precipitates with self-quenching fluorescence are frequently formed through $\pi-\pi$ aggregation of conjugated building blocks in water.[3] Therefore, utilization of noncovalent interactions to prepare well-defined nanostructures with highly fluorescent performance by self-assembly in water is a great challenge. Recently, Jayawickramarajah[4] and Ritter[5] have successfully prepared highly fluorescent nanowires through the self-assembly of β-cyclodextrin/adamantane (β-CD/AD = 1/1) host–guest couples in water.[6] However, the length of the reported self-assembled fluorescent nanowires with a few tens or hundreds of nanometers diameter, which generally reaches up to several micrometers, cannot be controlled effectively. Therefore, these reported nanowires can hardly be endocytosed by cells effectively due to their large size, which greatly limits their potential use in the biomedical fields in the future. Accordingly, to design and develop highly fluorescent nanoparticles for biological imaging techniques is quite urgent and indispensable. Previously, Rotello and co-workers[7] have developed a "bricks and mortar" approach to provide a general means for the controlled self-assembly of nanoparticles. In this strategy, the conformational flexibility of the polymers compensates for irregularities in the size and shape of the gold particle aggregate structure through complementary triple hydrogen-bonding recognition, allowing the efficient propagation of order during the self-assembly process. Recently, Tseng and co-workers[8] have improved this supramolecular strategy to obtain size-controlled water-soluble nanoparticles. In their design, the use of a capping/solvation group not only competes with the dendritic block to constrain the continuous propagation of the cross-linked network but also confers water solubility to the nanoparticles.

Herein, we employed this supramolecular strategy to achieve self-assembly of water-soluble supramolecular fluorescent nanoparticles (SFNPs) based on calcein fluorescent dye from four different molecular building blocks, namely: (1) AD-functionalized calcein, CA-AD, (2) β-CD-grafted branched polyethylenimine (M_w = 10 kDa), PEI-CD, (3) AD-functionalized polyethylene glycol (PEG) derivative (M_w = 2 kDa), mPEG-AD, and (4) AD-functionalized folate, FA-AD (Scheme 1). As expected, the resulting SFNPs display excellent fluorescent performance, improved physiological stability, and long-term systemic circulation time, as well as smart targeting capability for cancer-specific delivery.

Received: July 22, 2012
Accepted: September 24, 2012
Published: September 28, 2012

Scheme 1. Schematic Representation of Calcein-Based Supramolecular Fluorescent Nanoparticles (SFNPs) Self-Assembled in Water via Host−Guest Interactions of β-Cyclodextrin (β-CD) and Adamantane (AD)

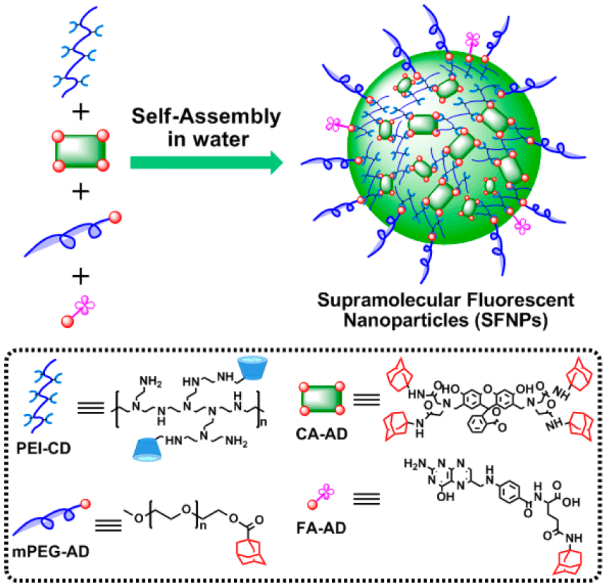

The synthetic procedure and characterization data of four building blocks CA-AD, PEI-CD, mPEG-AD, and FA-AD are described in the Supporting Information ([SI]). CA-AD with four AD units was first prepared through amidation of calcein with 1-adamantylamine in the presence of 1-ethyl-3-(3-dimethylaminopropyl) carbodiimide hydrochloride (EDC·HCl) and *N*-hydroxysuccinimide (NHS) (Scheme S1 and Figure S1, see the [SI]). PEI-CD was synthesized by a nucleophilic substitution reaction between 6-monotosyl β-CD and an amino group of PEI using potassium carbonate as the catalyst (Scheme S2, see the [SI]). For the PEI-CD molecule, there are about 25 β-CD recognition units grafted on a branched PEI backbone according to the ^{1}H NMR spectrum of Figure S2 (see the [SI]). Also, the successful preparation of mPEG-AD and FA-AD is clearly evidenced by ^{1}H NMR spectra of Figure S3 and Figure S4 (see the [SI]).

In contrast to a previous supramolecular strategy for preparation of water-soluble nanoparticles reported by Tseng and co-workers,[8] the uniqueness of our design is the use of a modified calcein (a fluorescent dye molecule) as the functionalized building block to endow the SFNPs with fluorescent performance. The solvation group of mPEG-AD not only competes with the building block of CA-AD to constrain the continuous propagation of the cross-linked network but also confers water solubility to the SFNPs.[9] Meanwhile, by tuning the mixing ratios of the CA-AD and PEI-CD building blocks in aqueous solution, the aggregation/segregation equilibrium of the cross-linked network fragments can be altered, allowing effective control over the sizes of the water-soluble SFNPs. As a result, the successful preparation of water-soluble SFNPs was confirmed by dynamic light scattering (DLS) and atomic force microscopy (AFM). As depicted in Figure 1A, with increasing molar ratio of CA-AD/PEI-CD from 1 to 8, the hydrodynamic diameter of the SFNPs varies from 100 to 150 nm (Figure S5, see the [SI]), which is consistent with the sizes of these nanoparticles in AFM images (Figure 1B and Figure 1C). In addition, it is worth noting that the introduction of folate into the SFNPs leads to a slight increase in its size.

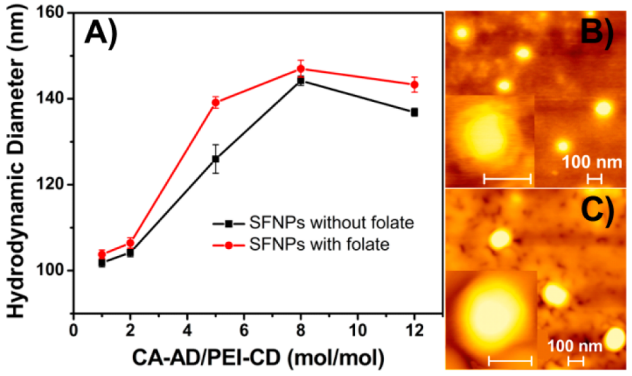

Figure 1. (A) Hydrodynamic diameter of SFNPs without or with folate as a function of CA-AD/PEI-CD molar ratio at room temperature. Red/black bars represent the mean values (n = 5). AFM images of SFNPs with the CA-AD/PEI-CD molar ratio of (B) 1 and (C) 8. The scale bars in the insetted images are 100 nm.

Although all of the SFNPs with different sizes exhibit good stability in deionized water, it is critical to examine the stability of the SFNPs under a physiological ionic strength to allow the use of the SFNPs in vivo. The results indicate that the SFNPs with the CA-AD/PEI-CD molar ratio of 1 and 2 exhibit good stability in PBS buffer (pH = 7.4), whereas the SFNPs with the CA-AD/PEI-CD molar ratio of more than 5 precipitate immediately in PBS buffer. It can be explained as follows: When the CA-AD/PEI-CD molar ratio is relatively high (more than 5), the excess AD groups of CA-AD cannot be effectively included in the cavity of CD groups of PEI-CD, which induces the unstable stacking structure formation in SFNPs. Thus, the high ionic strength of PBS buffer will destroy the structure of these SFNPs and further lead to the precipitation of these SFNPs in PBS buffer. Meanwhile, the incorporation of folate does not affect the stability of the SFNPs in PBS buffer. Furthermore, we employed real-time DLS measurements to monitor the size variation of SFNPs with the CA-AD/PEI-CD molar ratio of 1 under a physiological environment. As shown in Figure S6 ([SI]), both of the SFNPs without and with folate exhibit good stability in PBS buffer (pH = 7.4) at 37 °C.

The UV−vis measurement was performed to further confirm the formation of the SFNPs by self-assembly in water of the above four blocks. As shown in Figure 2A, the absorption band of CA-AD in $CHCl_3$ is centered at around 470 nm (Figure S7, see the [SI]). By comparison, the resulting SFNPs show an

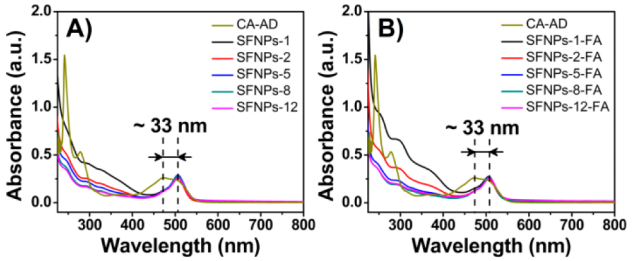

Figure 2. UV−vis spectra of (A) calcein-based SFNPs without folate and (B) calcein-based SFNPs with folate in deionized water and CA-AD in $CHCl_3$ at room temperature. The molar concentrations of CA-AD in SFNP aqueous solution and CA-AD in $CHCl_3$ were kept at 10 and 100 μM, respectively.

dx.doi.org/10.1021/mz300375c | *ACS Macro Lett.* 2012, 1, 1208−1211

increased absorption band accompanied by a remarkable bathochromic shift (~30 nm) to 500 nm, which can be attributed to the *J*-type aggregation[10] of calcein chromophores caused by the host−guest interaction of the CD unit in PEI-CD with an AD unit in CA-AD. Additionally, we note that the characteristic absorption band of the AD units from 250 to 450 nm broadens and weakens through the self-assembly. Meanwhile, with increasing molar ratio of CA-AD/PEI-CD from 1 to 8, the absorbance of the AD units in SFNP aqueous solution gradually decreases due to the reduced ratios of the AD units encapsulated into the hydrophobic cavity of CD. As shown in Figure 2B, similar results have been acquired with the introduction of folate into these SFNPs, suggesting that the outer layered folate groups do not affect the self-aggregation behavior of inner calcein chromophores.

Furthermore, we further investigated the fluorescent performance of the resultant SFNPs in water. In general, the $\pi-\pi$ stacking of most fluorescent dyes in water is the major reason for the fluorescence self-quenching.[3] To our surprise, the resulting SFNPs induced by self-aggregation of calcein chromophores in water through host−guest interaction exhibit strong green fluorescence without self-quenching, resulting from a great restriction of the quenching process by the CD units in SFNP aqueous solution.[11] In Figure 3, on one hand,

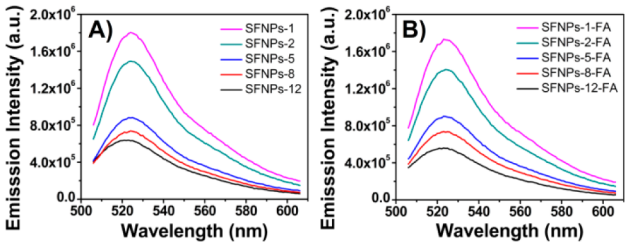

Figure 3. Fluorescence emission spectra (λ_{ex} = 491 nm) of (A) calcein-based SFNPs without folate and (B) calcein-based SFNPs with folate in deionized water at room temperature. The molar concentration of CA-AD in SFNP aqueous solution was kept at 10 μM.

the SFNPs with or without folate show nearly equivalent fluorescence emission intensity at about 525 nm, indicating that the incorporation of folate units would not change or even quench the fluorescence of calcein dyes in these nanoparticles. It can be attributed to the following two facts: First, the folate/calcein is not a donor/acceptor system, thus the folate will not quench the fluorescence of calcein dyes through the fluorescence resonance energy transfer (FRET) approach. Second, the outer-layered folate groups do not affect the self-aggregation behavior of inner-layered calcein chromophores or even quench their fluorescence. In addition, these SFNPs display a size-dependent fluorescent feature; that is, the fluorescence of the SFNPs decreases by a factor of about 3 with increasing size from ca. 100 nm to ca. 150 nm. The size-dependent fluorescent feature can be attributed to the fact that the increase of the CA-AD/PEI-CD molar ratio leads to the decrease in the number of the CA-AD encapsulated by the PEI-CD chain, which quenches the fluorescence of the SFNPs to some extent due to the $\pi-\pi$ stacking of unencapsulated calcein dyes in water.

To evaluate the cytotoxicity of the SFNPs with or without folate, the 3-(4,5-dimethylthiazol-2-yl)-2,5-diphenyltetrazolium bromide (MTT) method was performed in HeLa cells. Figure S8 (see the [SI]) demonstrates that the cell viability after 24 h incubation in HeLa cells is still above 40% when the final concentration of the SFNP aqueous solution reaches up to 0.5 mg/mL, illustrating the low cytotoxicity of the resulting SFNPs. The incorporation of folate into the SFNPs results in a slight increase of the cytotoxicity owing to their relatively high surface charge density of the SFNPs with folate, which can be directly confirmed by the zeta potential results in Figure S9 (see the [SI]). Meanwhile, an increased zeta potential for the calcein-based SFNPs in PBS buffer (pH 7.4) is observed by introduction of folate or increasing the CA-AD/PEI-CD molar ratio (Figure S9, see the [SI]).

The flow cytometry analysis was performed to further evaluate the cell internalization of the SFNPs by HeLa cells. Due to their own fluorescence, these SFNPs as a fluorescent probe were directly added to the culture medium, and the cells were incubated at 37 °C for the desired time. As depicted in Figure S10 (see the [SI]), the flow cytometry curves show that the relative fluorescence intensity of HeLa cells pretreated by the SFNPs with or without folate for only 5 min is surprisingly more than 100-fold of nonpretreated cells, and the fluorescence intensity just increases slightly with an increase of the incubation time, indicating the rapid cell internalization of the SFNPs by HeLa cells due to the cationic nature of these SFNPs. More importantly, the incorporation of folate groups further accelerates the cell internalization process of the SFNPs by HeLa cells. Moreover, the confocal laser scanning microscopy (CLSM) measurement was conducted to assess the imaging efficiency of these SFNPs in HeLa cells (Figure S11, see the [SI]). The HeLa cells with their cell nucleus stained by DAPI were incubated with the calcein-based SFNPs for 1 h. As a result, Figure 4 shows that the green fluorescence

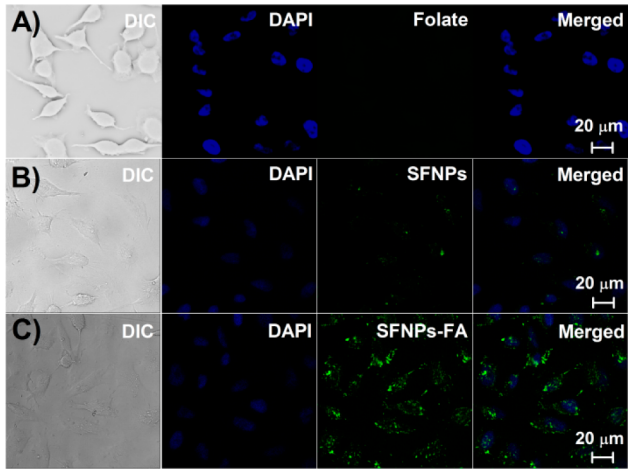

Figure 4. Confocal laser scanning microscopy (CLSM) images of HeLa cells that incubated with (A) excess folate, (B) calcein-based SFNPs without folate, and (C) calcein-based SFNPs with folate at 37 °C for 1 h with a final SFNP concentration of 10 μM. Cell nucleuses were stained with DAPI.

of the SFNPs mainly appears in the cytoplasm of HeLa cells, which indicates that the SFNPs are successfully internalized by HeLa cells and mainly reside in the cytoplasm.[12] As expected, the SFNPs with folate receptor (Figure 4C) exhibit much more excellent cancer imaging efficiency in contrast to the SFNPs without folate receptor (Figure 4B) due to the folate-mediated cancer cell targeting.[13]

dx.doi.org/10.1021/mz300375c | *ACS Macro Lett.* 2012, 1, 1208−1211

In conclusion, a novel class of calcein-based supramolecular fluorescent nanoparticles has been successfully prepared via a "bricks and mortar" strategy. The resulting supramolecular fluorescent nanoparticles, which exhibit not only a controllable nanoparticle size but also an excellent fluorescent performance with smart targeting capability for cancer-specific delivery, can be utilized for targeted cancer imaging. We envisage that this novel class of supramolecular fluorescent nanoparticles will open up a new approach to prepare highly fluorescent nanoparticles and can be further used in the living systems.

■ ASSOCIATED CONTENT

Supporting Information

Materials, methods, detailed experimental procedures, and supporting figures. This material is available free of charge via the Internet at http://pubs.acs.org.

■ AUTHOR INFORMATION

Corresponding Author

*E-mail: xyzhu@sjtu.edu.cn. Fax: +86-21-34205722. Tel: +86-21-34205699.

Notes

The authors declare no competing financial interest.

■ ACKNOWLEDGMENTS

This work is sponsored by the National Basic Research Program (2009CB930400, 2012CB821500), National Natural Science Foundation of China (20974062), and China National Funds for Distinguished Young Scientists (21025417).

■ REFERENCES

(1) (a) Whitesides, G. M.; Mathias, J. P.; Seto, C. T. *Science* **1991**, *254*, 1312. (b) Whitesides, G. M.; Grzybowski, B. *Science* **2002**, *295*, 2418. (c) Zhang, S. G. *Nat. Biotechnol.* **2003**, *21*, 1171.

(2) (a) Lehn, J. M. *Angew. Chem., Int. Ed.* **1990**, *29*, 1304. (b) Lehn, J. M. *Supramolecular Chemistry: Concepts and Perspectives*; VCH: Weinheim, Germany, 1995. (c) Ciferri, A. *Supramolecular Polymers*; Taylor & Francis: Boca Raton, FL, 2005. (d) Aida, T.; Meijer, E. W.; Stupp, S. I. *Science* **2012**, *335*, 813.

(3) (a) Luo, J.; Lei, T.; Wang, L.; Ma, Y.; Cao, Y.; Wang, J.; Pei, J. *J. Am. Chem. Soc.* **2009**, *131*, 2076. (b) Binder, W. H. *Angew. Chem., Int. Ed.* **2005**, *44*, 5172. (c) Tan, X.; Yang, G. *J. Phys. Chem. C* **2009**, *113*, 19926. (d) Ren, S.; Chen, S.; Jiang, M. *J. Polym. Sci., Part A* **2009**, *47*, 4267.

(4) Fathalla, M.; Neuberger, A.; Li, S.-C.; Schmehl, R.; Diebold, U.; Jayawickramarajah, J. *J. Am. Chem. Soc.* **2010**, *132*, 9966.

(5) Böhm, I.; Isenbügel, K.; Ritter, H.; Branscheid, R.; Kolb, U. *Angew. Chem., Int. Ed.* **2011**, *50*, 7407.

(6) (a) Huskens, J.; Deiji, M. A.; Reinhoudt, D. N. *Angew. Chem., Int. Ed.* **2002**, *41*, 4467. (b) Wenz, G.; Han, B.-H.; Müller, A. *Chem. Rev.* **2006**, *106*, 782. (c) Escalante, M.; Zhao, Y.; Ludden, M. J. W.; Vermeij, R.; Olsen, J. D.; Berenschot, E.; Hunter, C. N.; Huskens, J.; Subramaniam, V.; Otto, C. *J. Am. Chem. Soc.* **2008**, *130*, 8892. (d) Harada, A.; Hashidzume, A.; Yamaguchi, H.; Takashima, Y. *Chem. Rev.* **2009**, *109*, 5974. (e) Dong, R. J.; Zhou, L. Z.; Wu, J. L.; Tu, C. L.; Su, Y.; Zhu, B. S.; Gu, H. C.; Yan, D. Y.; Zhu, X. Y. *Chem. Commun.* **2011**, *47*, 5473.

(7) (a) Boal, A. K.; Ilhan, F.; DeRouchey, J. E.; Thurn-Albrecht, T.; Russell, T. P.; Rotello, V. M. *Nature* **2000**, *404*, 746. (b) Nandwana, V.; Subramani, C.; Eymur, S.; Yeh, Y.-C.; Tonga, G. Y.; Tonga, M.; Jeong, Y.; Yang, B.; Barnes, M. D.; Cooke, G.; Rotello, V. M. *Int. J. Mol. Sci.* **2011**, *12*, 6357.

(8) (a) Wang, H.; Wang, S.; Su, H.; Chen, K.-J.; Armijo, A. L.; Lin, W.-Y.; Wang, Y.; Sun, J.; Kamei, K.; Czernin, J.; Radu, C. G.; Tseng, H.-R. *Angew. Chem., Int. Ed.* **2009**, *48*, 4344. (b) Wang, S.; Chen, K.-J.; Wu, T.-H.; Wang, H.; Lin, W.-Y.; Ohashi, M.; Chiou, P.-Y.; Tseng, H.-R. *Angew. Chem., Int. Ed.* **2010**, *49*, 3777. (c) Liu, Y.; Wang, H.; Kamei, K.; Yan, M.; Chen, K.-J.; Yuan, Q.; Shi, L.; Lu, Y.; Tseng, H.-R. *Angew. Chem., Int. Ed.* **2011**, *50*, 3058.

(9) (a) Bellocq, N. C.; Kang, D. W.; Wang, X. H.; Jensen, G. S.; Pun, S. H.; Schluep, T.; Zepeda, M. L.; Davis, M. E. *Bioconjugate Chem.* **2004**, *15*, 1201. (b) Bartlett, D. W.; Su, H.; Hildebrandt, I. J.; Weber, W. A.; Davis, M. E. *Proc. Natl. Acad. Sci. U.S.A.* **2007**, *104*, 15549.

(10) (a) Gruszecki, W. I. *J. Biol. Phys.* **1991**, *18*, 99. (b) An, B.-K.; Kwon, S.-K.; Jung, S.-D.; Park, S. Y. *J. Am. Chem. Soc.* **2002**, *124*, 14410.

(11) (a) Coly, A.; Aaron, J.-J. *Anal. Chim. Acta* **1998**, *360*, 129. (b) Stone, M. T.; Anderson, H. L. *Chem. Commun.* **2007**, 2387.

(12) Madsen, J.; Armes, S. P.; Bertal, K.; MacNeil, S.; Lewis, A. L. *Biomacromolecules* **2009**, *10*, 1875.

(13) (a) Lee, R. J.; Low, P. S. *Biochim. Biophys. Acta* **1995**, *1233*, 134. (b) Wang, S.; Low, P. S. *J. Controlled Release* **1998**, *53*, 39. (c) Yoo, H. S.; Park, T. G. *J. Controlled Release* **2004**, *96*, 273. (d) Hilgenbrink, A. R.; Low, P. S. *J. Pharm. Sci.* **2005**, *94*, 2135. (e) Bae, Y.; Jang, W.-D.; Nishiyama, N.; Fukushima, S.; Kataoka, K. *Mol. BioSyst.* **2005**, *1*, 24.